





Multi-sensor, multi-scale, Bayesian data synthesis for mapping within-year wildfire progression

Morgan A. Crowley ^a, Jeffrey A. Cardille ^a, Joanne C. White ^b
and Michael A. Wulder ^b

^aDepartment of Natural Resource Sciences, McGill University, Ste.-Anne-de-Bellevue, Québec, Canada;

^bCanadian Forest Service (Pacific Forestry Centre), Natural Resources Canada, Victoria, British Columbia, Canada

ABSTRACT

As freely available remotely sensed data sources proliferate, the ability to combine imagery with high spatial and temporal resolutions enables applications aimed at near-term disturbance detection. In this case study, we present methods for synthesizing burned-area information from multiple sources to map the active phase of the Elephant Hill fire from the 2017 fire season in British Columbia. We used the Bayesian Updating of Land Cover (BULC) algorithm to merge burned-area classifications from a range of remote-sensing sources such as Landsat-8, Sentinel-2, and MODIS. We created provisional classifications by comparing the post-fire Normalized Burn Ratio against pre-fire image composite within the fire boundary provided by the Province of British Columbia. BULC fused the classifications in Google Earth Engine, producing a cohesive time-series stack with updated burned areas for 19 distinct days. The fire burned unevenly throughout its lifespan: a rapid burn phase of 53,097 ha in two weeks by late July, a steady burn phase to 60,000 ha until late August, an accelerated burn phase of 95,766 ha until mid-September, and containment at 203,560 ha in October. The highly automated methods presented herein can synthesize multi-source fire classifications for active phase monitoring both retrospectively and in near-real-time.

ARTICLE HISTORY

Received 1 May 2018

Accepted 6 October 2018

1. Introduction

Forest disturbance mapping has been made possible for Canada through the Composite-to-Change (C2C) protocol, which uses annual proxy best-available-pixel (BAP) composites across the 30 m Landsat record (Hermosilla et al. 2016, 2017; White et al. 2017). BAP composites enable cloud and gap-free observations while ensuring that similar illumination and growing conditions (August 1 ± 30 days) are represented across years (White et al. 2014). Using these data, the average area burned annually by wildfire in Canada (1985–2010) is estimated to be 1.6 Mha ($\sigma = 1.1$ Mha, where σ denotes the standard deviation). Operationally, annual data is acquired by provincial and territorial fire management agencies to track the location, size, and cause of wildfires, among

CONTACT Morgan A. Crowley  morgan.crowley@mail.mcgill.ca  Department of Natural Resource Sciences, McGill University, 21,111 Lakeshore Road, Ste.-Anne-de-Bellevue, Québec, Canada

© 2018 The Author(s). Published by Informa UK Limited, trading as Taylor & Francis Group.

This is an Open Access article distributed under the terms of the Creative Commons Attribution-NonCommercial-NoDerivatives License (<http://creativecommons.org/licenses/by-nc-nd/4.0/>), which permits non-commercial re-use, distribution, and reproduction in any medium, provided the original work is properly cited, and is not altered, transformed, or built upon in any way.

other attributes. These jurisdictional data are compiled with other sources to produce the Canadian National Fire Database (CNFDB; Amiro et al. 2001; Stocks et al. 2003; Parisien et al. 2006; Burton et al. 2008). The CNFDB, which typically does not exclude unburned islands and water bodies from its fire perimeters, estimates an average annual area burned of 2.3 Mha ($\sigma = 1.9$ Mha; White et al. 2017). While both C2C and CNFDB provide estimates of burned area, there are opportunities to augment and further refine burned-area estimates using data from multiple earth observing satellites.

Individual sensors have been used to detect characteristics of forest fires, creating retrospective maps of burned area at a variety of spatial resolutions. For example, the MODIS Collection 6 MCD64A1 global burned area product provides geographic locations and timing of fires at 500 m spatial resolution derived using a burn-sensitive vegetation index (Giglio et al. 2015; Humber et al. 2018). MODIS-derived products provide high temporal but low spatial resolution for monitoring fires, and spatial interpolation techniques have been used to downscale its coarse resolution for fire analyses across North American forests (de Groot et al. 2007; de Groot, Pritchard, and Lynham 2009; Parisien et al. 2011; Parks, Parisien, and Miller 2012; Parks 2014). For Canadian boreal forests, the Normalized Burn Ratios (NBR) and the differenced pre-disturbance and post-disturbance NBRs (dNBR) are reliable estimators of burned areas (Key and Benson 2006; Hall et al. 2008; Soverel, Perrakis, and Coops 2010; Soverel et al. 2011; Hermosilla et al. 2016, 2017; White et al. 2017; Frazier et al. 2018). The NBR and dNBR have been used with fine-scale Landsat time series to detect stand-replacing fires in Canadian forested ecosystems at annual time steps (e.g., Schroeder et al. 2011; Hermosilla et al. 2016, 2017; San-Miguel, Andison, and Coops 2017; White et al. 2017; Frazier et al. 2018; San-Miguel, Andison, and Coops 2018). In a few cases, observations from multiple sensors have been combined to enable retrospective mapping. For example, the dNBR can be calculated from pre-fire Landsat-8 and post-fire Sentinel-2 observations (Quintano, Fernández-Manso, and Fernández-Manso 2018). These retrospective maps of extinguished fires are useful for managers (Roy et al. 2005; Lentile et al. 2006; San-Miguel, Andison, and Coops 2017), but the rapid spread and associated smoky conditions render near-term classification of a fire's rapidly changing extent difficult.

Recent developments suggest that information from multiple satellites can be combined at greater temporal resolution not only for retrospective mapping but also for estimating fire growth while the fire is still active. Until very recently, the density of available data was such that fine-scale near-real-time monitoring of fires was impractical due to high costs and sparse frequencies of observations. Fusing observations from multiple sources advance the possibility of monitoring in near-real-time (Li and Roy 2017; Wulder et al. 2018), such as during the active phase of fires. The Bayesian Updating of Land Cover (BULC) algorithm synthesizes classifications of individual images through time by weighing evidence from multiple classifications to produce a time series of land undergoing rapid change (Cardille and Fortin 2016). BULC records the land-use land-cover (LULC) history for each class of stability and change across large areas, allowing users to view the trajectory and probability of any pixel in the image calculated using Bayes' Theorem. In this letter, we demonstrate how combining observations from multiple sensors can facilitate the mapping of active fires. This fusion takes advantage of the growing frequency and quality of sensors with different spectral and spatial characteristics, capturing near-real-time growth patterns of long-lived fires to inform managers and planners interested in fire risk, spread, and impact.

2. Materials and Methods

2.1. Study Area

The 2017 fire season was the largest on record for British Columbia (BC) and mapping these fires is important for monitoring forest-disturbance impacts, with considerations related to timber supply, carbon consequences, and animal habitat. One of the largest fires was the Elephant Hill fire, also known as the Ashcroft fire (K20637). This fire started on 11 July 2017 north of Ashcroft, British Columbia and was contained by October 2. The Elephant Hill fire's eventual perimeter grew to 511 km, based upon data shared by the British Columbia Wildfire Service. The final burned area within this perimeter was reported to be 192,016 ha, damaging infrastructure in addition to forested lands (BC Wildfire Service 2017a, 2017b). For context, the final burned area of this individual fire was two-thirds of the cumulative burned area for the entire 2015 fire season (280,738 ha burned by 1,858 fires), and double that of the total area burned in the 2016 fire season (102,019 ha burned by 1,050 fires; BC Wildfire Service 2017c).

2.2. Provisional classifications using Landsat-8 OLI, Sentinel-2 and MODIS

Images intersecting the Elephant Hill fire perimeter from summer and autumn 2017 were identified for classification in Google Earth Engine, a cloud-based platform for accessing and processing satellite imagery and geospatial datasets (Gorelick et al. 2017). Differences over the dNBR threshold outlined in Hall et al. (2008) were classified as 'Burned/Burning'; those below the threshold were classified as 'Unburned' at that time step (e.g., Frazier et al. 2018). The treatment of each of the relevant sensors – Landsat-8, Sentinel-2, and MODIS – differed slightly and are described below.

Landsat-8: We computed the pre-fire NBR using a 2016 BAP gap-free reflectance composite that was generated following the C2C approach (e.g., White et al. 2014, 2017; Hermosilla et al. 2016, 2017). To compare with the pre-fire status, we identified 10 Landsat-8 surface reflectance images from six different dates, with each image having less than 10% cloud cover. We masked clouds and haze before classification using the pixel-level Quality Assurance (QA) band (Zhu 2017; Egorov et al. 2018; USGS 2018). We differenced the NBR of each image with the pre-fire NBR to produce six dated provisional classifications for use in BULC.

Sentinel-2: We identified 33 Sentinel-2 (A and B) images with less than 10% cloud cover on 11 distinct dates, for classification and use in BULC. In Earth Engine, we generated a pre-fire best-available-pixel image using similar pixel selection criteria as used in C2C. We then calculated the pre-fire NBR values for each pixel for comparison to each image's post-fire NBR values. Because observations from Sentinel-2 are provided in UTM tiles smaller than the study area, we mosaicked the Sentinel-2 images for each distinct day before classification then masked clouds and haze using the QA band of Sentinel-2 observations. The result was 11 date-specific classifications that were used as inputs in BULC.

MODIS: We identified monthly summaries of burned areas from the MODIS Collection 6 MCD64A1 burned area product, for classification and use in BULC (Giglio et al. 2015; Humber et al. 2018). This raster data product detects day-of-burning globally at 500 m resolution with an average uncertainty of 4.3 days and a processing delay between 1.5 to 3 months for the Elephant Hill fire. Because the burned-area product contains the detected burn date in

each of the three monthly images, we reclassified these MODIS burned-area products into Burned/Burning and Unburned layers in 15-day summaries. The result was six date-specific summary classifications that were used as inputs to BULC.

Across the three sources, there were 23 provisional classifications of burned area from 19 distinct imaging dates during the study period. Using observations from multiple remote sensing sources greatly reduced the revised interval considered across the portfolio of sensors., we were able to increase the frequency of observations to reduce the temporal revisit intervals provided by the sensors (e.g., Li and Roy 2017). The six Landsat-8 surface reflectance classifications, eleven Sentinel-2 classifications, and six MODIS bi-weekly classifications were ordered by date and used as provisional classification inputs in the BULC algorithm for the Elephant Hill fire study area, outlined in Table 1. The combined sensors imaged each pixel an average of 19.5 times between July 5 and October 30, with the entire study area having been imaged at least once in 13 of the 15 weeks that the fire burned.

2.3. BULC

To synthesize the information from these three different sensors, we used the BULC algorithm (Cardille and Fortin 2016). BULC applies Bayes’ Theorem to interpret a series of time-ordered provisional classifications, synthesizing a time series that shows change and stability in the study area at the per-pixel level. To gauge the reliability of a given provisional classification to the construction of the time series, BULC compares each new classification – from any data source – against the previous classification in the time stack. Using the Producer’s Accuracy as the conditional probabilities in Bayes’ Theorem, BULC traces the probability of both classes through time. As detailed in Cardille and Fortin (2016), BULC can synthesize moderate-quality classifications over short time intervals to track rapidly changing landscapes. BULC tolerates occasional errors (i.e., resulting from smoke, clouds), and is thereby an ideal fusion algorithm for active-phase fire classification. BULC is able to quantify the burned and burning area of a fire at intermediate time steps between the beginning and end of individual fire events utilizing the dense stack of relatively clear provisional classifications from Landsat-8, Sentinel-2, and MODIS in Google Earth Engine.

3. Results

The Elephant Hill fire burned unevenly throughout its active phase: rapid escalation in late July, slow and steady growth until late August, an accelerated phase until mid-September, and containment by October (Figure 1).

BULC synthesizes provisional input classifications from the active phase of the fire, which allows per-pixel burn detection within the British Columbia fire-event perimeter at the

Table 1. Satellite source and acquisition dates for Elephant Hill fire observations, whether MODIS, Landsat-8, or Sentinel-2, that were used as inputs in BULC.

	July				August						September					October			
	5	14	20	30	4	6	11	19	22	26	3	15	16	18	28	3	5	10	30
Landsat-8	X	X		X		X			X				X						
Sentinel-2					X	X	X			X		X			X	X	X	X	X
MODIS	X		X		X			X			X			X					

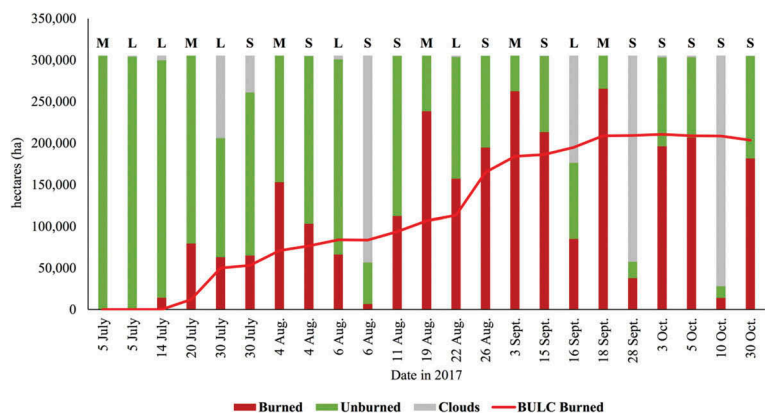


Figure 1. Growth in Elephant Hill burned area through time as synthesized in BULC from Landsat-8 (L), Sentinel-2 (S), and MODIS (M). The line indicates BULC estimated Burned/Burning area through time, while bars show the high variability among provisional classifications from each sensor.

collection date of each event. **Figure 2** shows the final fire perimeter delineated by the British Columbia Wildfire Service superimposed on the BULC burned-area estimates for the Elephant Hill fire at the following time steps: July 5 (a), July 30 (b), August 26 (c), and October 30 following 100% containment (d). **Figure 2(b)** is the product of five images over 3.5 weeks and shows fire growth from 461 ha on July 20 to 50,122 ha on July 30. **Figure 2(c)** shows the BULC classification that results in 14 images over 7.5 weeks, showing a fire growth from 113,103 ha on August 22 to 164,738 ha on August 26. **Figure 2(d)** shows the final BULC classification of Burned/Burning pixels within the BC polygon after the fire had been 100% contained. The BULC Burned/Burning area covers 67% of the British Columbia fire agency polygon, amounting to 203,560 burned ha, 6% higher than the estimated 192,016 burned ha (BC Wildfire Service 2017a, 2017b).

The BULC fire classifications detect unburned pixels within the BC fire perimeter. **Figure 3** compares zoomed regions of the final MODIS burned-area summary with the

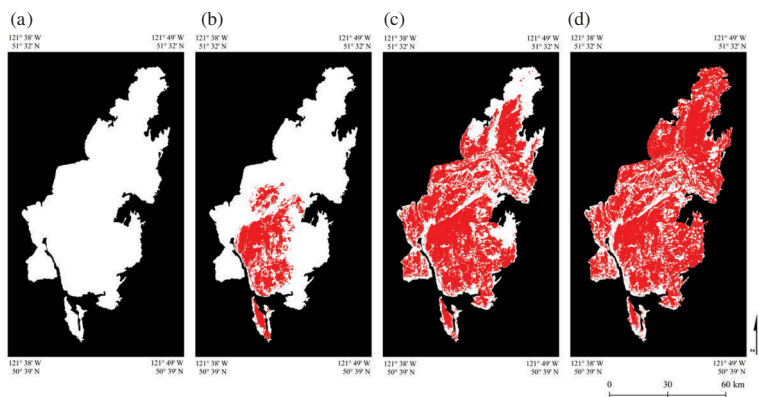


Figure 2. BULC burned-area classification estimates in red within the BC Elephant Hill fire perimeter on dates July 5 (a), July 30 (b), August 26 (c), October 30 (d).

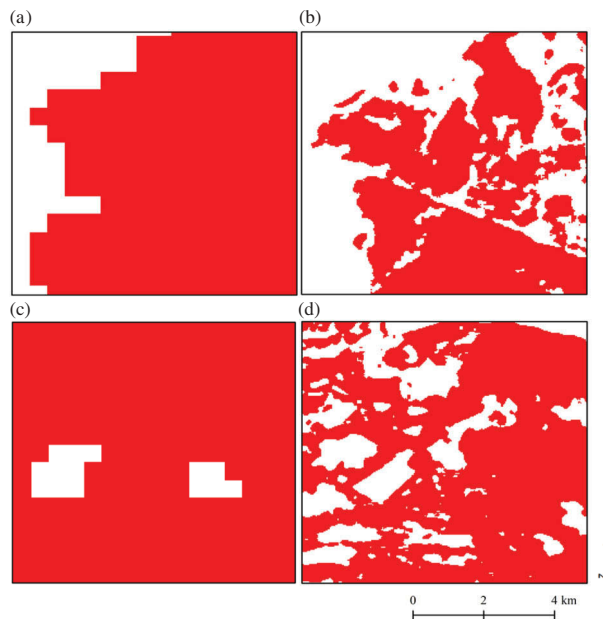


Figure 3. Post-fire, final MODIS Collection 6 MCD64A1 burned pixels zoomed to 500 m following 30 October 2017 centred on $121^{\circ} 29' \text{ W}$, $50^{\circ} 55' \text{ N}$ (a) compared with the final BULC classification (b); post-fire, final MODIS Collection 6 MCD64A1 burned pixels centred on $121^{\circ} 9' \text{ W}$, $51^{\circ} 0' \text{ N}$ (c) compared with the final BULC classification (d). The multi-sensor approach of the final BULC classification refines the edges of both burned and unburned objects present in the coarser MODIS Collection 6 MCD64A1 dataset.

final BULC classifications for the Elephant Hill fire. The MODIS burned area shown in [Figure 3\(a\)](#) compared with the final BULC classification shown in [Figure 3\(b\)](#) emphasizes the unburned pixels within the fire-event perimeter. Additionally, based upon inputs from Landsat and Sentinel-2, BULC identifies Burned/Burning pixels at a finer spatial resolution than the MODIS dataset. The MODIS burned area, shown in [Figure 3\(c\)](#), detects unburned pixels with a coarser resolution than the fine spatial resolution of the final BULC classification in [Figure 3\(d\)](#).

As BULC processed provisional input classifications, the new information contained therein updated the synthesized classification of the burned area, as shown in [Figure 4](#). As the fire progressed through the area surrounding -120.933 , 51.286 , MODIS-based provisional classification from September 3 changed the probability of fire from around 38 to 62%, high enough to tip the estimated LULC to Burned/Burning in [Figure 4\(a\)](#). The next view of the area, Sentinel-based provisional classification from September 15 confirmed most of the September 3 classification and changed the probabilities of many of the pixels to be 70% in [Figure 4\(b\)](#), which classified the LULC to Burned/Burning in those corresponding pixels. The subsequent view of the area (imperfect Landsat-based provisional classification from September 16) refined the BULC classification further. The newly burned pixels in the northwest had a probability of being Burned/Burning around 58% and therefore were captured as Burned/Burning in the BULC classification, and the nearby pixels in the southwest that had not been classified as Burned/Burning were between 24 and 44% probability in [Figure 4\(c\)](#).

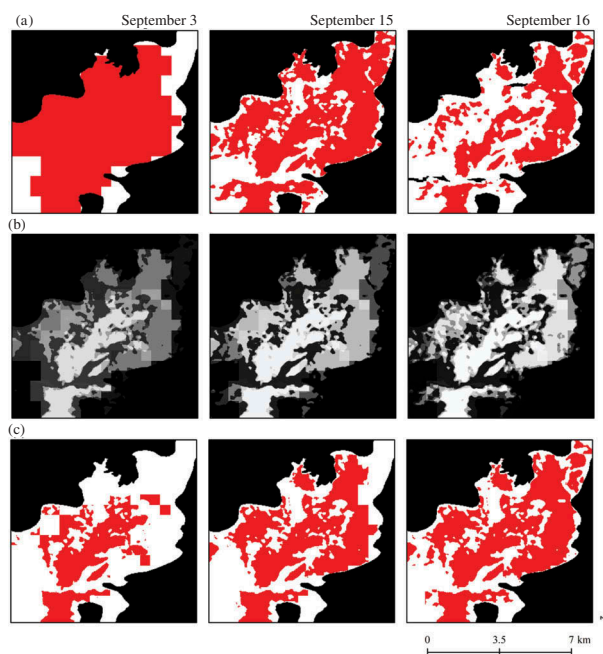


Figure 4. As the fire progresses in this region (zoomed on 120° 59' W, 51° 17' N) from September 3 to September 16, the imperfect provisional classifications in row (a) provide evidence of Burned/Burning to influence the per-pixel probabilities in row (b) (lighter gradient depicts larger probabilities), and the updated probabilities classify the pixels as Burned/Burning in the BULC classification in row (c).

4. Discussion

In this study, we have demonstrated a highly automated approach for combining accessible data products for active fire monitoring. The application of the BULC algorithm on dNBR and other burned-area classifications provides a seamless and multi-sensor method for synthesis of burned-area observations. This method combines observations from disparate data sources to increase the frequency of useable images to work towards near-real-time detection of burned areas during the fire's active phase. Additional methodological novelty is demonstrated by the capacity to increase temporal revisit rates supporting the reconstruction of active fire lifespans to better understand fire growth and underlying drivers with high temporal frequency and fine spatial resolution.

In this case study, we found that observations from each sensor contributed to the time series tracking the growth of the Elephant Hill fire, thus supporting the fusion of multi-sensor observations to expand near-real-time burned-area detection (Hilker et al. 2009a, 2009b; Wulder et al. 2010; Li and Roy 2017; Wulder et al. 2018). Relying exclusively on Landsat-8 input classifications, our fire time series would be limited to burn detection primarily early in the active fire phase. Similarly, using only input classifications from Sentinel-2, the fire time step would be limited to burn detection after the first major growth in late July. Lastly, utilizing only MODIS burned area data would have caused over-classification of burned areas with coarse pixel resolution (Fraser et al. 2004; White et al. 2017). Even though BULC was able to create a credible time series using these sources, it was not quite real-time mapping: the density of data limited the BULC classification of the fire's burned area to about a 1-week delay. Because BULC

is not limited to any set of sensors, as additional imagery becomes available the time series can become more narrowly timed, perhaps to a sub-weekly time series.

The findings of this research provide a method for synthesizing burned-area classifications from multiple sources with varying scales and resolutions, including single-date remote sensing, burned-area detection algorithms, and jurisdictionally produced fire perimeters. For reconstructing the British Columbia 2017 fire season, there are observations available from other platforms (e.g., Landsat-7, Sentinel-3) that BULC could also incorporate imagery to create a sub-weekly time series. Due to the portability of the post-classification synthesis approach presented, future studies can apply these methods to create temporally dense fire-classification stacks for burned-area detection whether analysing fires in near-real-time or retrospectively.

Acknowledgments

This research was undertaken as part of the 'Earth Observation to Inform Canada's Climate Change Agenda (EO3C)' project jointly funded by the Canadian Space Agency (CSA), Government Related Initiatives Program (GRIP), and the Canadian Forest Service (CFS) of Natural Resources Canada. This research was enabled in part by support provided by WestGrid (www.westgrid.ca) and Compute Canada (www.computecanada.ca).

ORCID

Morgan A. Crowley  <http://orcid.org/0000-0001-5946-529X>
 Jeffrey A. Cardille  <http://orcid.org/0000-0002-4667-9085>
 Joanne C. White  <http://orcid.org/0000-0003-4674-0373>
 Michael A. Wulder  <http://orcid.org/0000-0002-6942-1896>

References

- Amiro, B. D., J. B. Todd, B. M. Wotton, K. A. Logan, M. D. Flannigan, B. J. Stocks, J. A. Mason, D. L. Martell, and K. G. Hirsch. 2001. "Direct Carbon Emissions from Canadian Forest Fires, 1959 to 1999." *Canadian Journal of Forest Research* 31: 512–525. doi:10.1139/x00-197.
- BC Wildfire Service. 2017a. "Wildfires of Note - Elephant Hill (K20637)." <http://bcfireinfo.for.gov.bc.ca/hprScripts/WildfireNews/OneFire.asp?ID=620>
- BC Wildfire Service. 2017b. "Prot_Current_Fire_Polys_Sp" (dataset). Ministry of Forests, Lands, Natural Resource Operations and Rural Development. Accessed January 25 2018. <https://catalogue.data.gov.bc.ca/dataset/fire-perimeters-current>.
- BC Wildfire Service. 2017c. "Wildfire Season Summary." <https://www2.gov.bc.ca/gov/content/safety/wildfire-status/about-bcws/wildfire-history/wildfire-season-summary>
- Burton, P. J., M. A. Parisien, J. A. Hicke, R. J. Hall, and J. T. Freeburn. 2008. "Large Fires as Agents of Ecological Diversity in the North American Boreal Forest." *International Journal of Wildland Fire* 17 (6): 754–767. doi:10.1071/WF07149.
- Cardille, J. A., and J. Fortin. 2016. "Bayesian Updating of Land Cover Estimates in a Data-Rich Environment." *Remote Sensing of Environment* 186: 234–249. doi:10.1016/j.rse.2016.08.021.
- de Groot, W. J., R. Landry, W. A. Kurz, K. R. Anderson, P. Englefield, R. H. Fraser, R. J. Hall, et al. 2007. "Estimating Direct Carbon Emissions from Canadian Wildland Fires." *International Journal of Wildland Fire* 16: 593–606. doi:10.1071/WF06150.
- de Groot, W. J., J. M. Pritchard, and T. J. Lynham. 2009. "Forest Floor Fuel Consumption and Carbon Emissions in Canadian Boreal Forest Fires." *Canadian Journal of Forest Research* 39: 367–382. doi:10.1139/X08-192.

- Egorov, A. V., D. P. Roy, H. K. Zhang, M. C. Hansen, and A. Kommareddy. 2018. "Demonstration of Percent Tree Cover Mapping Using Landsat Analysis Ready Data (ARD) and Sensitivity with respect to Landsat ARD Processing Level." *Remote Sensing* 10 (2): 209. doi:10.3390/rs10020209.
- Fraser, R. H., R. J. Hall, R. Landry, T. Lynham, D. Raymond, B. Lee, and Z. Li. 2004. "Validation and Calibration of Canada-Wide Coarse Resolution Satellite Burned-Area Maps." *Photogrammetric Engineering & Remote Sensing* 70: 451–460. doi:10.14358/PERS.70.4.451.
- Frazier, R. J., N. C. Coops, M. A. Wulder, T. Hermosilla, and J. C. White. 2018. "Analyzing Spatial and Temporal Variability in Short-Term Rates of Post-Fire Vegetation Return from Landsat Time Series." *Remote Sensing of Environment* 205: 32–45. doi:10.1016/j.rse.2017.11.007.
- Giglio, L., C. Justice, L. Boschetti, and D. Roy. 2015. "MCD64A1 MODIS/Terra+Aqua Burned Area Monthly L3 Global 500m SIN Grid V006" (dataset). NASA EOSDIS Land Processes DAAC. Accessed March 1, 2018. <https://doi.org/10.5067/MODIS/MCD64A1.006>.
- Gorelick, N., M. Hancher, M. Dixon, S. Ilyushchenko, D. Thau, and R. Moore. 2017. "Google Earth Engine: Planetary-Scale Geospatial Analysis for Everyone." *Remote Sensing of Environment* 202: 18–27. doi:10.1016/j.rse.2017.06.031.
- Hall, R. J., J. T. Freeburn, W. J. de Groot, J. M. Pritchard, T. J. Lynham, and R. Landry. 2008. "Remote Sensing of Burn Severity: Experience from Western Canada Boreal Fires." *International Journal of Wildland Fire* 17 (4): 476–489. doi:10.1071/WF08013.
- Hermosilla, T., M. A. Wulder, J. C. White, N. C. Coops, and G. W. Hobart. 2017. "Updating Landsat Time Series of Surface-Reflectance Composites and Forest Change Products with New Observations." *International Journal of Applied Earth Observation and Geoinformation* 63: 104–111. doi:10.1016/j.jag.2017.07.013.
- Hermosilla, T., M. A. Wulder, J. C. White, N. C. Coops, G. W. Hobart, and L. B. Campbell. 2016. "Mass Data Processing of Time Series Landsat Imagery: Pixels to Data Products for Forest Monitoring." *International Journal of Digital Earth* 9 (11): 1035–1054. doi:10.1080/17538947.2016.1187673.
- Hilker, T., M. A. Wulder, N. C. Coops, J. Linke, G. McDermid, J. G. Masek, F. Gao, and J. C. White. 2009a. "A New Data Fusion Model for High Spatial-And Temporal-Resolution Mapping of Forest Disturbance Based on Landsat and MODIS." *Remote Sensing of Environment* 113 (8): 1613–1627. doi:10.1016/j.rse.2009.03.007.
- Hilker, T., M. A. Wulder, N. C. Coops, N. Seitz, J. C. White, F. Gao, J. G. Masek, and G. Stenhouse. 2009b. "Generation of Dense Time Series Synthetic Landsat Data through Data Blending with MODIS Using a Spatial and Temporal Adaptive Reflectance Fusion Model." *Remote Sensing of Environment* 113 (9): 1988–1999. doi:10.1016/j.rse.2009.05.011.
- Humber, M. L., L. Boschetti, L. Giglio, and C. O. Justice. 2018. "Spatial and Temporal Intercomparison of Four Global Burned Area Products." *International Journal of Digital Earth* 1–25. doi:10.1080/17538947.2018.1433727.
- Key, C. H., and N. C. Benson. 2006. "Landscape Assessment: Sampling and Analysis Methods." *General Technical Report RMRS-GTR-164-CD*. Fort Collins, CO: US Department of Agriculture, Forest Service, Rocky Mountain Research Station.
- Lentile, L. B., Z. A. Holden, A. M. Smith, M. J. Falkowski, A. T. Hudak, P. Morgan, S. A. Lewis, P. E. Gessler, and N. C. Benson. 2006. "Remote Sensing Techniques to Assess Active Fire Characteristics and Post-Fire Effects." *International Journal of Wildland Fire* 15 (3): 319–345. doi:10.1071/WF05097.
- Li, J., and D. P. Roy. 2017. "A Global Analysis of Sentinel-2A, Sentinel-2B and Landsat-8 Data Revisit Intervals and Implications for Terrestrial Monitoring." *Remote Sensing* 9 (9): 902. doi:10.3390/rs9090902.
- Parisien, M. A., S. A. Parks, C. Miller, M. A. Krawchuk, M. Heathcott, and M. A. Moritz. 2011. "Contributions of Ignitions, Fuels, and Weather to the Burn Probability of a Boreal Landscape." *Ecosystems* 14: 1141–1155. doi:10.1007/S10021-011-9474-2.
- Parisien, M. A., V. S. Peters, Y. Wang, J. M. Little, E. M. Bosch, and B. J. Stocks. 2006. "Spatial Patterns of Forest Fires in Canada 1980–1999." *International Journal of Wildland Fire* 15: 361–374. doi:10.1071/WF06009.
- Parks, S. A. 2014. "Mapping Day-Of-Burning with Coarse-Resolution Satellite Fire-Detection Data." *International Journal of Wildland Fire* 23: 215–223. doi:10.1071/WF13138.

- Parks, S. A., M. A. Parisien, and C. Miller. 2012. "Spatial Bottom-Up Controls on Fire Likelihood Vary across Western North America." *Ecosphere* 3: 12. doi:10.1890/ES11-00298.1.
- Quintano, C., A. Fernández-Manso, and O. Fernández-Manso. 2018. "Combination of Landsat and Sentinel-2 MSI Data for Initial Assessing of Burn Severity." *International Journal of Applied Earth Observation and Geoinformation* 64: 221–225. doi:10.1016/j.jag.2017.09.014.
- Roy, D. P., Y. Jin, P. E. Lewis, and C. O. Justice. 2005. "Prototyping a Global Algorithm for Systematic Fire-Affected Area Mapping Using MODIS Time Series Data." *Remote Sensing of Environment* 97 (2): 137–162. doi:10.1016/j.rse.2005.04.007.
- San-Miguel, I., D. W. Anderson, and N. C. Coops. 2017. "Characterizing Historical Fire Patterns as a Guide for Harvesting Planning Using Landscape Metrics Derived from Long Term Satellite Imagery." *Forest Ecology and Management* 399: 155–165. doi:10.1016/j.foreco.2017.05.021.
- San-Miguel, I., D. W. Anderson, and N. C. Coops. 2018. "Quantifying Local Fire Regimes Using the Landsat Data-Archive: A Conceptual Framework to Derive Detailed Fire Pattern Metrics from Pixel-Level Information." *International Journal of Digital Earth*. doi:10.1080/17538947.2018.1464072.
- Schroeder, T. A., M. A. Wulder, S. P. Healey, and G. G. Moisen. 2011. "Mapping Wildfire and Clearcut Harvest Disturbances in Boreal Forests with Landsat Time Series Data." *Remote Sensing of Environment* 115 (6): 1421–1433. doi:10.1016/j.rse.2011.01.022.
- Soverel, N. O., N. C. Coops, D. D. Perrakis, L. D. Daniels, and S. E. Gergel. 2011. "The Transferability of a dNBR-derived Model to Predict Burn Severity across 10 Wildland Fires in Western Canada." *International Journal of Wildland Fire* 20 (4): 518–531. doi:10.1071/WF10081.
- Soverel, N. O., D. D. Perrakis, and N. C. Coops. 2010. "Estimating Burn Severity from Landsat dNBR and RdNBR Indices across Western Canada." *Remote Sensing of Environment* 114 (9): 1896–1909. doi:10.1016/j.rse.2010.03.013.
- Stocks, B. J., J. A. Mason, J. B. Todd, E. M. Bosch, B. M. Wotton, B. D. Amiro, M. D. Flannigan, et al. 2003. "Large Forest Fires in Canada, 1959–1997." *Journal of Geophysical Research* 108 (D1: FFR5): 1–12. doi:10.1029/2001JD000484.
- U. S. Geological Survey. 2018. *U.S. Landsat Analysis Ready Data (ARD) Data Format Control Book (DFCB)*. LSDS-809. Sioux Falls, SD: US Department of Interior, Earth Resources Observation and Science (EROS) Center. Accessed April 15 2018. https://landsat.usgs.gov/sites/default/files/documents/LSDS-1873_US_Landsat_ARD_DFCB.pdf.
- White, J. C., M. A. Wulder, T. Hermosilla, N. C. Coops, and G. W. Hobart. 2017. "A Nationwide Annual Characterization of 25-Years of Forest Disturbance and Recovery for Canada Using Landsat Time Series." *Remote Sensing of Environment* 194: 303–321. doi:10.1016/j.rse.2017.03.035.
- White, J. C., M. A. Wulder, G. W. Hobart, J. E. Luther, T. Hermosilla, P. Griffiths, N. C. Coops, et al. 2014. "Pixel-Based Image Compositing for Large-Area Dense Time Series Applications and Science." *Canadian Journal of Remote Sensing* 40 (3): 192–212. doi:10.1080/07038992.2014.945827.
- Wulder, M. A., N. C. Coops, D. P. Roy, J. C. White, and T. Hermosilla. 2018. "Land Cover 2.0." *International Journal of Remote Sensing* 39 (12): 4254–4284. doi:10.1080/01431161.2018.1452075.
- Wulder, M. A., J. C. White, M. D. Gillis, N. Walsworth, M. C. Hansen, and P. Potapov. 2010. "Multiscale Satellite and Spatial Information and Analysis Framework in Support of a Large-Area Forest Monitoring and Inventory Update." *Environmental Monitoring and Assessment* 170 (1–4): 417–433. doi:10.1007/s10661-009-1243-8.
- Zhu, Z. 2017. "Change Detection Using Landsat Time Series: A Review of Frequencies, Preprocessing, Algorithms, and Applications." *ISPRS Journal of Photogrammetry and Remote Sensing* 130: 370–384. doi:10.1016/j.isprsjprs.2017.06.013.